Counting Bungarotoxin Binding Sites of Nicotinic Acetylcholine Receptors in Mammalian Cells with High Signal/Noise Ratios

Paul D. Simonson,[†] Hannah A. DeBerg,[†] Pinghua Ge,[†] John K. Alexander,[‡] Okunola Jeyifous,[‡] William N. Green,[‡] and Paul R. Selvin[†]*
[†]Department of Physics and the Center for the Physics of Living Cells, University of Illinois at Urbana-Champaign, Urbana, Illinois; and
[‡]Department of Neurobiology, University of Chicago, Chicago, Illinois

ABSTRACT   Nicotinic acetylcholine receptors are some of the most studied synaptic proteins; however, many questions remain that can only be answered using single molecule approaches. Here we report our results from single $\alpha7$ and neuromuscular junction type nicotinic acetylcholine receptors in mammalian cell membranes. By labeling the receptors with fluorophore-labeled bungarotoxin, we can image individual receptors and count the number of bungarotoxin-binding sites in receptors expressed in HEK 293 cells. Our results indicate that there are two bungarotoxin-binding sites in neuromuscular junction receptors, as expected, and five in $\alpha7$ receptors, clarifying previous uncertainty. This demonstrates a valuable technique for counting subunits in membrane-bound proteins at the single molecule level, with nonspecialized optics and with higher signal/noise ratios than previous fluorescent protein-based techniques.

The ability to count the number of ligand binding sites or subunits in single, membrane-bound receptors in mammalian cells with a high signal/noise ratio is useful for many ion channel applications (1–3). By fluorescently labeling and exciting the ion channel, the number of ligand binding sites can be determined by counting the number of staircased photobleaching events, which occur randomly in time. Ulbrich and Isacoff (1), for example, used this approach to determine that NMDA receptors containing NR1 and NR3B subunits, expressed in *Xenopus* oocytes and labeled with fluorescent proteins (GFP or dsTomato), have a 2:2 subunit stoichiometry. Their experiments, however, required extra care to achieve good signal/noise. The relatively poor signal/noise ratio of the fluorescent proteins necessitated the use of a 1.65 NA objective, quartz coverslips, and specialized immersion oil. Cell fixation, however, was not required because the channels were stationary in *Xenopus* oocytes.

Ji et al. (3) were able to extend the technique to mammalian cells to count subunits in calcium channels. They used a 1.45 NA objective, which did not require a special coverslip or immersion oil. Using GFP, however, led to low signal/noise ratios and made counting the number of photobleaching steps ambiguous in >50% of the spots analyzed. Furthermore, cell fixation was required.

Dye photobleaching has also been used to count pRNAs in viral DNA packaging motors (4,5), subunits in amyloid oligomers spin-coated on glass (6), and leukocidin and α-hemolysin subunits in receptors on glass (7).

Here we demonstrate a method to label nicotinic acetylcholine receptors (nAChRs) in cells using external fluorophores that are extremely bright and photostable, thereby avoiding the difficulties with using fluorescent proteins in cells (4). We used fluorophore-bungarotoxin (BgT)

conjugates to label the receptors and observe the stepwise photobleaching behavior. The nAChRs used include neuromuscular junction (NMJ) nAChRs, which have two BgT-binding sites (BBSs) (8,9) and are useful for technique verification, and $\alpha7$ nAChRs, for which the number of BBSs is unclear—either four or five (10,11).

We incubated HEK 293 cells, which were transiently transfected with subunits composing NMJ nAChRs, with BgT conjugated to Alexa647. This was followed by cell fixation and imaging using total internal reflection fluorescence microscopy (see the Supporting Material). An oxygen scavenging system was used to increase photostability of the dyes (12). We also attempted to label nontransfected HEK293 cells and saw no labeled receptors, confirming the specificity of BgT for the nAChRs.

Cells with labeled receptors were clearly discernible from background. Software was used to automatically detect each spot and output its fluorescence-intensity-versus-time trace. The numbers of photobleaching steps were counted "by eye," meaning we used a step-fitting program to initially fit the steps and then rejected very small steps or corrected for steps that were obviously missed (see Fig. S4 in the Supporting Material). Ambiguous traces that did not show clear photobleaching steps were rejected. We found that many traces showed one- and two-step photobleaching, and a rather insignificant number showed more than two photobleaching steps (Fig. 1). The traces with more than two photobleaching steps are likely due to two or more nAChRs, or

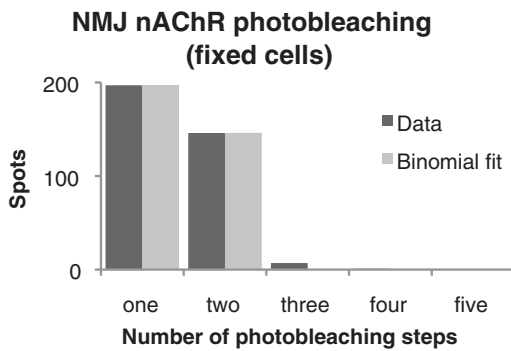## NMJ nAChR photobleaching (fixed cells)

FIGURE 1 Histogram of photobleaching steps for NMJ type nAChRs. The histogram suggests that there are indeed only two BBSs in this receptor.

a receptor with a nearby nonspecifically bound fluorophore, being within the radius of a diffraction-limited spot. In an effort to reject as many of these types of spots as possible, the center of a spot was tracked by fitting its image to a two-dimensional Gaussian. Spots were rejected that showed sudden position shifts >15 nm that were coincident with a photobleaching step because these spots were likely to contain more than one receptor. By fitting the histogram to a binomial distribution with two possible BBSs, we estimated that the portion of sites labeled with active fluorophores was ~60%.

In contrast to NMJ nAChRs, the number of BBSs and general structure of α7 nAChRs are not well characterized, although it is established that α7 nAChRs are homopentamers (13). Rangwala et al. (10) suggested that there are fewer than five BBSs in the α7 receptor, based on alkylation of the sites using bromoACh techniques. The data suggested that the number of BBSs might be reduced from five binding sites due to post-translational modification of the α7 subunits, causing differences in α7 subunits within the homopentamer (10).

To determine the actual number of BBSs in α7 nAChRs, we labeled the receptors with Alexa647-BgT and counted the number of BBSs using the same methods as those used for NMJ nAChRs. A slight difficulty is that the α7 nAChR is not normally transported to the cell membrane without coexpression of ric-3 (14). Instead of cotransfecting cells with ric-3 and α7 plasmid DNA, we used a chimera of α7 and 5HT3 (serotonin receptor) that is transported to the cell surface without the presence of ric-3. Insertion of 5HT3 did not affect the bungarotoxin-binding properties of the receptor because the extracellular, N-terminal BgT-binding portion of the α7 subunit, which contains the identical sequence to the BgT binding portion of AChBP (15,16), is included in the chimera (10,13). The chimera has also previously been shown to have indistinguishable pharmacology from the full-length α7 for several ligands and binds bungarotoxin (10,13). We transiently transfected HEK 293 cells with the α7-5HT3 construct and proceeded with labeling, fixing, and imaging. We found a significant
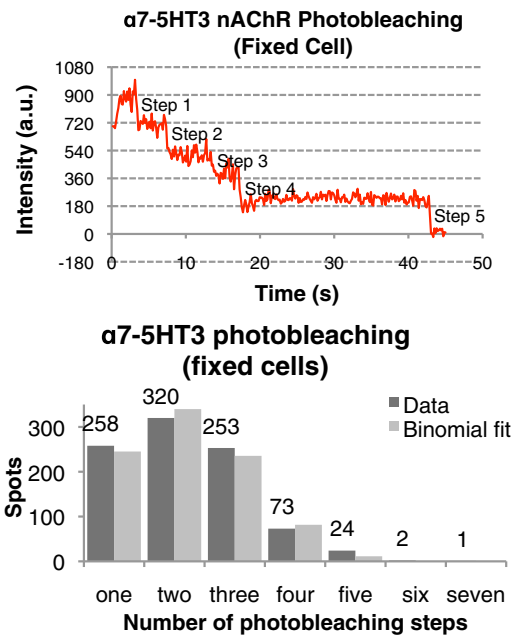
α7-5HT3 nAChR Photobleaching (Fixed Cell)

α7-5HT3 photobleaching (fixed cells)

FIGURE 2 (*Top*) Photobleaching trace of α7-5HT3 receptor labeled with BgT-Alexa647. (*Bottom*) Histogram of number of photobleaching steps per labeled receptor and binomial distribution fit.

number of α7-5HT3 receptors with five or fewer photobleaching steps (Fig. 2), and a much smaller number with six or more photobleaching steps. We postulated that five-step photobleaching was indicative of α7 receptors having five BBSs, although we cannot formally rule out the possibility of an additional subpopulation of receptors containing four or fewer BBSs. Fitting the resulting histogram to a binomial distribution suggested that our labeling efficiency was 41%.

As mentioned, our technique gives a drastic improvement in signal/noise ratio over similar techniques that use GFP to label subunits. For example, receptors with singly labeled Alexa647s emitted four times more total photons than single GFPs (data not shown). We also collected α7 data using a 1.65 N.A. objective (see the Supporting Material). There was no significant increase in the signal/noise with the external fluorophores, although the 1.65 N.A. did help for GFP-labeled receptors, increasing the number of collected photons (data not shown). Alexa647 is also red-shifted compared to GFP, which helps with cell autofluorescence problems.

This higher signal/noise ratio allows us to achieve a higher spatiotemporal resolution that is necessary for tracking receptors that are diffusing in a nonfixed cell membrane, while still counting BBSs. We found that for nonfixed cells, the labeled α7-5HT3 receptors had a two-dimensional diffusion coefficient of 0.1 μm^2 s^{-1}. This required tracking in order to see photobleaching steps (Fig. 3). To count the number of photobleaching steps of diffusing receptors, it is necessary to completely photobleach the receptors quickly. This is because the receptors should not cross paths,
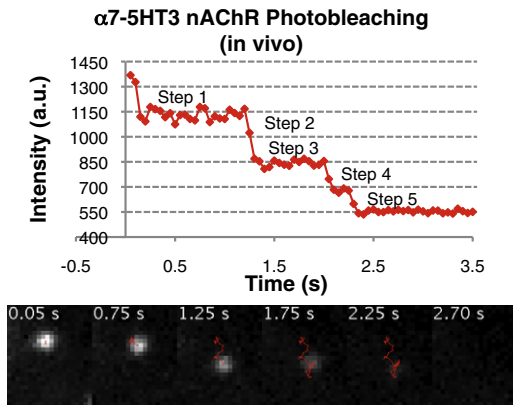
α7-5HT3 nAChR Photobleaching (in vivo)

FIGURE 3 In vivo photobleaching of an α7-5HT3 nAChR. In the photobleaching trace (*top*), the labeled receptor appears to have five attached fluorophores: one fluorophore photobleaches near 0.15 s, two photobleach simultaneously near 1.25 s, a fourth photobleaches near 2 s, and the last photobleaches near 2.3 s. Because of diffusion, the receptor had to be tracked (see *bottom image sequence*).

which will tend to obfuscate which receptor is which after the crossing. Also, the receptors must not travel in domains in the membrane that are far away or close enough to the coverslip surface to make a significant change in the total internal reflection excitation power applied to the fluorophores. We used a high laser intensity (though not fluorophore-saturating) and acquired images at 0.05 s per frame. The signal/noise ratio was high enough to see stepwise photobleaching in a few diffusing receptors, although we were unable to make out clear steps in most of the live-cell traces. Due to the simplicity of analyzing nondiffusing receptors, we did most of our measurements in fixed cells.

In conclusion, we have used fluorophore-BgT conjugates to count the number of bungarotoxin binding sites in NMJ and α7-5HT3 nAChRs. We confirmed that NMJ receptors have two bungarotoxin binding sites, and we found α7-5HT3 receptors to have five. We found that the high signal/noise ratios allow for counting subunits, sometimes even in receptors that are diffusing in nonfixed cell membranes. In addition, the use of BgT for labeling receptors is not limited to nAChRs with natural binding sites. Indeed, short amino-acid sequences have been inserted into other proteins and shown to induce BgT binding (17). Thus, the techniques reported here should prove useful for other membrane-bound protein studies in both fixed and nonfixed mammalian cells.

SUPPORTING MATERIAL

Four figures and nine equations are available at http://www.biophysj.org/biophysj/supplemental/S0006-3495(10)01110-0.

REFERENCES and FOOTNOTES

1. Ulbrich, M. H., and E. Y. Isacoff. 2007. Subunit counting in membrane-bound proteins. *Nat. Methods.* 4:319–321.

2. Ulbrich, M. H., and E. Y. Isacoff. 2008. Rules of engagement for NMDA receptor subunits. *Proc. Natl. Acad. Sci. USA.* 105:14163–14168.

3. Ji, W., P. Xu, …, L. Chen. 2008. Functional stoichiometry of the unitary calcium-release-activated calcium channel. *Proc. Natl. Acad. Sci. USA.* 105:13668–13673.

4. Nashmi, R., M. E. Dickinson, …, H. A. Lester. 2003. Assembly of α4β2 nicotinic acetylcholine receptors assessed with functional fluorescently labeled subunits: effects of localization, trafficking, and nicotine-induced upregulation in clonal mammalian cells and in cultured midbrain neurons. *J. Neurosci.* 23:11554–11567.

5. Shu, D., H. Zhang, …, P. Guo. 2007. Counting of six pRNAs of φ29 DNA-packaging motor with customized single-molecule dual-view system. *EMBO J.* 26:527–537.

6. Ding, H., P. T. Wong, …, D. G. Steel. 2009. Determination of the oligomer size of amyloidogenic protein β-amyloid(1–40) by single-molecule spectroscopy. *Biophys. J.* 97:912–921.

7. Das, S. K., M. Darshi, …, H. Bayley. 2007. Membrane protein stoichiometry determined from the step-wise photobleaching of dye-labeled subunits. *ChemBioChem.* 8:994–999.

8. Karlin, A., and M. H. Akabas. 1995. Toward a structural basis for the function of nicotinic acetylcholine receptors and their cousins. *Neuron.* 15:1231–1244.

9. Pantoja, R., E. A. Rodriguez, …, H. A. Lester. 2009. Single-molecule imaging of a fluorescent unnatural amino acid incorporated into nicotinic receptors. *Biophys. J.* 96:226–237.

10. Rangwala, F., R. C. Drisdel, …, W. N. Green. 1997. Neuronal α-bungarotoxin receptors differ structurally from other nicotinic acetylcholine receptors. *J. Neurosci.* 17:8201–8212.

11. Palma, E., S. Bertrand, …, D. Bertrand. 1996. Neuronal nicotinic α7 receptor expressed in *Xenopus* oocytes presents five putative binding sites for methyllycaconitine. *J. Physiol.* 491:151–161.

12. Aitken, C. E., R. A. Marshall, and J. D. Puglisi. 2008. An oxygen scavenging system for improvement of dye stability in single-molecule fluorescence experiments. *Biophys. J.* 94:1826–1835.

13. Drisdel, R. C., and W. N. Green. 2000. Neuronal α-bungarotoxin receptors are α7 subunit homomers. *J. Neurosci.* 20:133–139.

14. Williams, M. E., B. Burton, …, J. Aiyar. 2005. Ric-3 promotes functional expression of the nicotinic acetylcholine receptor α7 subunit in mammalian cells. *J. Biol. Chem.* 280:1257–1263.

15. Unwin, N. 2005. Refined structure of the nicotinic acetylcholine receptor at 4 Å resolution. *J. Mol. Biol.* 346:967–989.

16. Dellisanti, C. D., Y. Yao, …, L. Chen. 2007. Crystal structure of the extracellular domain of nAChR α1 bound to α-bungarotoxin at 1.94 Å resolution. *Nat. Neurosci.* 10:953–962.

17. Sekine-Aizawa, Y., and R. L. Huganir. 2004. Imaging of receptor trafficking by using α-bungarotoxin-binding-site-tagged receptors. *Proc. Natl. Acad. Sci. USA.* 101:17114–17119.